# Adaptive Nonlinear Projective Filtering
## *Application to Filtering of Artifacts in EEG Signals*

Bartosz Binias and Michał Niezabitowski
*Silesian University of Technology, Faculty of Automatic Control, Electronics and Computer Science, Akademicka 16 Street, 44-100, Gliwice, Poland*

Keywords: EEG, Electroencephalography, Adaptive Filtering, Artifact Filtering, Artifact Correction, Signal Reconstruction, Nonlinear Projective Filtering, Nonlinear State Space Projection, Biomedical Signals.

Abstract: In this work a novel approach to filtering of eyeblink related artifacts from EEG signals is presented. Proposed solution, the Adaptive Nonlinear Projective Filtering (ANPF) algorithm, combines the classic approach to adaptive filtering with algorithms from nonlinear state space projection family. Performance of described method is compared with adaptive filter based on Normalized Least Mean Squares algorithm in terms of median Normalized Mean Squared Error. Data used in conducted research was simulated according to described procedure. Such approach allowed for a reliable comparison and evaluation of algorithm's signal correction properties. Additionally, a real time modification of ANPF algorithm is proposed and tested. The analysis of sensitivity to changes of parameter values was also performed. Achieved results were tested for statistical significance. According to obtained scores ANPF significantly outperforms referential method during offline processing.

## 1 INTRODUCTION

Artifacts related with eye movements are among the most significant sources of noise and contamination of electroencephalographic (EEG) data. Because the frequency characteristics of ocular artifacts tend to overlap with those of EEG, they make an analysis of such signals not only less effective but, in many cases, impossible (R. J. Croft, 2000; Correa et al., 2007). Apart from frequency mixing this kind of contamination is usually characterised by amplitudes that are several times higher than typical range of useful EEG signals. This results in a very low signal-to-noise (SNR) ratio that makes this problem even more demanding. Most commonly implemented approach to dealing with contaminated segments of signal is simply removing them from further analysis (Jung et al., 2000; R. J. Croft, 2000). However, such approach leads to a significant loss of data which, is unacceptable in e.g. real-time analysis of EEG signal for Brain-Computer Interface (BCI) applications (Binias et al., 2016b). Another very popular branch of approaches is based on adaptive filtering algorithms applied either in time or frequency domain (Jung et al., 2000; Binias et al., 2015; Binias et al., 2016b). These methods require that at least one regressing channel is provided. The most common source of such information is an electrooculogram (EOG) recording, which can serve as reference for regression-based algorithms (Jung et al., 2000). Although capable of producing a very good results in attenuation of ocular artifacts, potential of these methods is weakened by big sensitivity to changes of some parameters, that may result even in destabilization of the whole filtering process (Haykin and Widrow, 2003). Among other techniques of filtering eyeblink related contamination mentioned can be methods based on blind source separation. Those include Principal Component Analysis (PCA) and Independent Component Analysis (ICA) which rely on recorded EEG and EOG signals for calibration (P. Berg, 1991; Jung et al., 2000). Especially, the ICA method when applied to large number of data recorded over many channels, can produce results of high quality. However, it must be noted that this method works best in semi-automatic approach, where supervision of experienced user (i.e. expert) is required (Makeig et al., 2000). The concept of nonlinear filtering of time series by locally linear phase space projections has been derived using concepts from deterministic dynamical systems, or chaos theory (Schreiber and Kantz, 1998). Such methods will be referred to as Nonlinear Projective Filtering (NFP) in this work. Although NFP was designed for the purpose of filtering signals that are deterministically chaotic, this approach has been successfully implemented for applications requiring de-



Binias, B. and Niezabitowski, M.
Adaptive Nonlinear Projective Filtering - Application to Filtering of Artifacts in EEG Signals.
DOI: 10.5220/0006414604400448
In *Proceedings of the 14th International Conference on Informatics in Control, Automation and Robotics (ICINCO 2017) - Volume 1*, pages 440-448
ISBN: 978-989-758-263-9

noising of biomedical signals such as electrocardiogram (ECG) and EEG (Kantz and Schreiber, 1998; Richter et al., 1998; Kotas, 2009; Kotas, 2004; Gao et al., 2011). NFP based approaches rely on phase space reconstructions performed under Takens' conditions (Takens, 1981). This theorem has been also effectively utilized in analysis of nonlinear time series. An example of such signals are, for instance, various components of eye movement (Harezlak, 2017).

In this work a novel algorithm - the Adaptive Nonlinear Projective Filtering (ANPF) is proposed and validated for applications of artifact filtering in EEG signals. Method is compared with adaptive filter based on Normalized Least Mean Squares (NLMS) algorithm in terms of median Normalized Mean Squared Error (NMSE). Additionally, a real time modification of ANPF algorithm is proposed and tested.

## 2 MATERIALS

Evaluation of eye blink correction and filtering artifacts in EEG signals is inextricably linked with the problem of selection of a proper referential, uncontaminated signal. Since EEG signals are recorded with the disturbance already additively mixed, there is no precise way to extract the original, desired component. Two approaches to that problem can be mentioned here. First one is based on the use of real EEG recordings (Binias et al., 2016b). This approach relies on time indexes marked by researchers. However, since these are mostly subjective, only approximate information of method's accuracy is provided. Additionally, since it is impossible to recover the exact morphology of uncontaminated signal, there is no unambiguous way of evaluating how accurate was reconstruction of the filtered signal. A second approach to described problem requires use of simulated EEG data (Binias et al., 2015). Since both artifact-free EEG and additive artifact components are available, it is possible to reliably evaluate artifact filtering and signal correction methods. This can be achieved e.q. by comparing the original, uncontaminated EEG data with filtered signal. This approach was utilized in this research.

EEG signals are characterized by low amplitudes (normally in range from 0.5 to 100 $\mu V$)and bandwidth mostly located below 100 $Hz$ (Binias et al., 2015). Some characteristic frequency ranges can be distinguished from EEG recordings. These are often referred to as brainwaves (Teplan, 2002; Nunez and Srinivasan, 2006; da Silva, 1991). Delta (below 3 $Hz$) waves are commonly associated with deep sleep (Teplan, 2002). Although, theta activity ($3-7$ $Hz$) has been observed during cognitive visual processing (Grunwald et al., 1999) it is generally attributed to states of drowsiness. States of wakeful relaxation, or tiredness are dominated by alpha waves ($8-12$ $Hz$). This activity can also be increased by closing eyes (Teplan, 2002; da Silva, 1991). Normal waking consciousness, alertness and an active concentration are related to beta range ($13-29$ $Hz$) (Teplan, 2002; Craig et al., 2012). The role of gamma waves (over 30 $Hz$) remains an active topic of a research. EEG signal $s(n)$ can be modelled as an additive mixture of $K$ sinusoidal components oscillating with frequencies $f_k$, which are evenly distributed across given frequency range starting at 0 $Hz$ and ending at $F_{lim} = 100$ $Hz$. In this work $K = 200$. Let us assume that $\phi_k$ is the pseudorandomly generated initial phase of *k-th* frequency component of $s(n)$, $n$ is a discrete time index and $w_a(k)$ is the amplitude of said component. Then, the equation used for generation of simulated EEG time series can be formulated as in (1)

$$y(n) = \sum_{k=1}^{K} w_a(k) sin(2\pi f_k n + \phi_k). \quad (1)$$

To ensure that the power spectrum density function of simulated output will be similar to that of realistic EEG, signal amplitudes of each frequency component were chosen accordingly to a typical power spectrum characteristics of EEG signals. In general, it can be assumed that during states of focused relaxation, alpha activity will be dominant with some small beta influence (Teplan, 2002; Binias et al., 2015). Therefore, amplitudes $w_a$ of the individual frequency components can be approximated by normal distribution with mean value randomly selected from alpha wave range $\mu_f = 8-12$ $Hz$ and standard deviation $\sigma_f$ adjusted so that the maximal value equals to $F_{lim} = 100$ $Hz$ (Binias et al., 2015). For the simulation purposes all frequency values lower than zero were rejected. Then, for remaining frequencies formula (1) was applied. An exemplary relation between amplitudes and frequencies of simulated EEG signals is presented in Fig. 1. A comparison of simulated EEG time course with a real one is shown in Fig. 2. Presented exemplary signal was recorded accordingly to procedure utilized for the purpose of different research (Binias et al., 2016a).

Three main types of eye movement related artifacts in EEG can be distinguished. These are eye blinks, eye movements (saccades) and scalp or facial muscle contractions (short time, high amplitude spikes) (Binias et al., 2015). This research is entirely focused on eye blink artifacts. Morphology of such contamination is shown in Fig. 3. Presented exem-

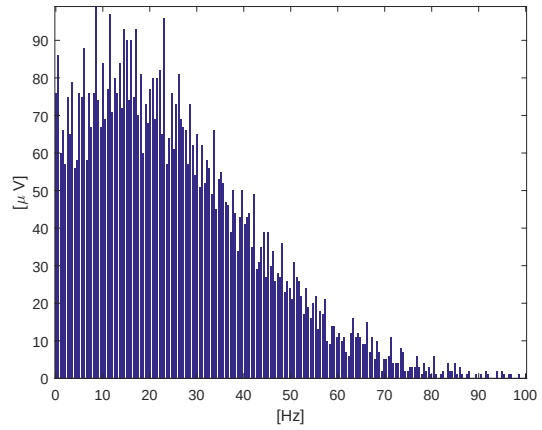


Figure 1: Exemplary relation between amplitudes and frequencies of simulated EEG signals (own source).

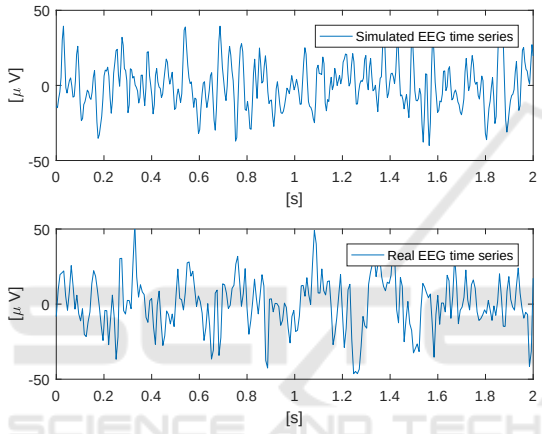


Figure 2: Examples of simulated and real EEG time courses (own source).

plary signal was recorded accordingly to procedure utilized for the purpose of different research (Binias et al., 2016a).

In this work, morphology of such artifacts has been approximated by function presented in (2). An exemplary time course of that function is shown in Fig. 4:

$$b(n) = w_b U\Big(\frac{n}{\sigma_b\sqrt{2\pi}} e^{-\frac{1}{2}(\frac{n-\mu_b}{\sigma_b})^2}\Big). \qquad (2)$$

In formula (2) $n \in < -N_0/2; N_0/2 >$ is a discrete time variable. If total duration of simulation is denoted by $T_0$ and sampling frequency is represented by $f_s$, then $N_0 = f_s T_0$ ($T_0 = 1\ s$ and $f_s = 200\ Hz$ in this work). Mean of Gaussian distribution function $\mu_b$ was set to 0 for all simulations ($\mu_b = 0\ s$). Standard deviation $\sigma_b$ controls the time positions of simulated blink peaks and thus is responsible for the duration of simulated eyeblink artifact. Relation between defined parameters and morphology of simulated artifact is presented in Fig. 4.

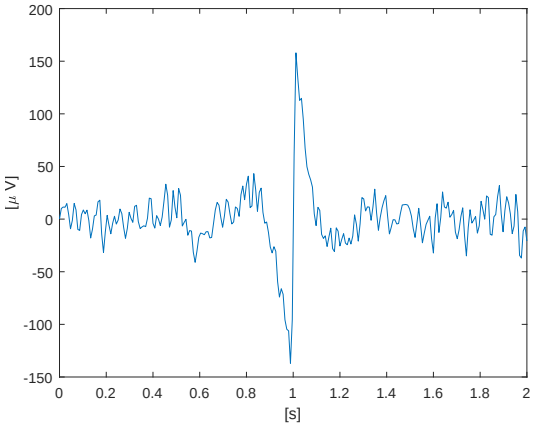


Figure 3: Real EEG signal contaminated by eye blink artifact (Binias et al., 2016a) (own source).

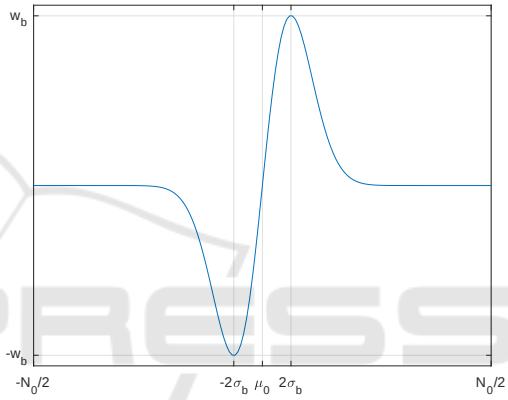


Figure 4: Time course of simulated eye blink artifact (own source).

According to experimental work, such artifacts can be divided into three categories basing on their length: short blinks ($71-100$ ms), medium blinks ($101-170$ ms) and long blinks ($171-300$ ms) (Benedetto et al., 2011). Therefore, parameter $\sigma_b$ was randomly selected from uniform distribution ranged $\sigma_b \in < 0.035\ s; 0.085\ s >$ that corresponds with short blink duration. $U(f)$ is introduced as a normalization operator of function $f$. As a result its application range of function is normalized to range $f \in < -1; 1 >$. The amplitude of simulated artifact was controlled by parameter $w_b$ which was randomly selected from uniform distribution $w_b \in < 70\ \mu V; 110\ \mu V >$ (based on (Binias et al., 2015)). Obtained simulated eye blink was ten amplified and added to original, uncontaminated EEG signal $s(n)$ as in (3). The scaling coefficient $w_m$ was selected randomly for each test from uniform distribution ranged from 0.8 to 1.0 ($w_m \in < 0.8; 1.0 >$). The introduction of scaling of $b(n)$ signals originates from biophysical aspect of the problem. The bioelectrical source of eye blink artifacts is located closer to position of electrode record-

ing reference signal than to EEG measurement locations. Therefore, amplitudes of such artifacts will be, in general, lower in EEG channels than in EOG. A model of additive source mixing and linear scaling is commonly accepted among researchers (Nunez et al., 1997; Pfurtscheller and Da Silva, 1999; Blankertz et al., 2008)

$$x(n) = s(n) + w_m b(n). \tag{3}$$

All simulation parameters used in this work were selected on the basis of literature review (Binias et al., 2015; Benedetto et al., 2011). That way the most realistic characteristics of simulated time series could be ensured. Time course of simulated EEG signal with eye blink artifact contamination and overlapped referential EOG recording are presented in Fig. 5. The referential EOG signal that was provided with the simulated data was obtained from adding a pink noise to the $b(n)$.

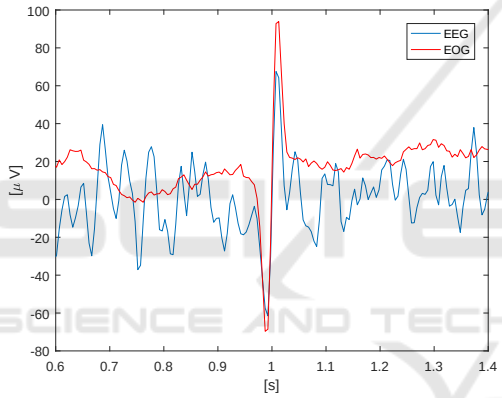


Figure 5: Time courses of simulated EEG signal with eye blink artifact contamination and referential EOG recording (own source).

# 3 METHODS

## 3.1 Nonlinear Projective Filtering

A discrete time series $s(n) \in \mathbb{R}^N$ can be represented as a trajectory in a $D$-dimensional phase space with Takens Method using time delay coordinates $s(n) = \left[s(n), s(n+\tau), \ldots, s(n+(D-1)\tau)\right]$ ($D$ denotes the embedding dimension, $\tau$ is a delay time) (Takens, 1981). For deterministic dynamical systems the phase trajectory is frequently confined to a set of points in state space, referred to as the attractor. Simplest approach to the problem of denoising or filtering of the contaminated signals in the phase space can be reduced to the following steps (Kantz and Schreiber, 1998; Schreiber and Kantz, 1998):

1. obtain a referential, desired trajectory, which is a low dimensional approximation of the attractor;
2. project each point in the trajectory of the contaminated signal $s(n)$ orthogonally on to the approximation of the attractor to produce a trajectory vector of cleaned time series $\hat{s}(n)$;
3. convert the filtered phase space trajectory $\hat{s}(n)$ to the scalar time domain to produce a denoised time series $\hat{s}(n)$.

The described Nonlinear Projective Filtering algorithm was designed for the filtering of various types of noise contamination present in deterministically chaotic systems.

## 3.2 Adaptive Nonlinear Projective Filtering

The goal of proposed, novel algorithm is the elimination of eye-blink related artifacts from EEG signals. Although in this application the eye-blink component $b(n)$ is a disturbance, from the signal-to-noise ratio perspective it is much easier to solve the inverse problem. Therefore, the proposed ANPF will first try to find the estimate of eye-blink component in contaminated EEG signal $\hat{b}(n) \simeq w_m b(n)$ by filtering out all EEG related components. The difference $e(n)$ between recorded, noisy EEG signal $x(n)$ and filtered eye-blink artifact $\hat{b}(n)$ will be an estimate of clear, uncontaminated signal $s(n)$. Mathematically, this can be described as in (4)

$$\begin{aligned} e(n) &= x(n) - \hat{b}(n), \\ e(n) &= s(n) + w_m b(n) - \hat{b}(n), \\ e(n) &\simeq s(n). \end{aligned} \tag{4}$$

For the ANPF algorithm to work properly a reliable low dimensional approximation to the attractor must be provide. This approximation will be also referred to as a reference trajectory. Together with EEG, the EOG signals are often recorded. These signals are measured from locations that lay close to location of bioelectrical sources of eye blink and movement related artifacts (i.e. eyes). EOG is commonly used as a secondary noise input for the adaptive noise cancelling algorithms (Binias et al., 2015; Binias et al., 2016b). The reconstructed state space trajectory of simulated EOG signal $b_r(n)$ will be used as the referential approximation of the attractor in this work.

Considering the presented assumptions and considerations, the ANPF algorithm can be realized in following steps:

1. create a state space representation of contaminated EEG signal $x(n)$ and reference EOG trajectory $b_r(n)$;
2. for each every point in contaminated trajectory find closest point of reference trajectory;
3. replace a corrected point from contaminated trajectory with its closest point from reference trajectory to produce a cleaned vector $\hat{b}(n)$;
4. convert the cleaned trajectory of $\hat{b}(n)$ to scalar time domain.
5. subtract cleaned reference trajectory $\hat{b}(n)$ from contaminated signal $x(n)$ in time domain to obtain a filtered EEG signal $e(n)$.

In Fig. 6 presented are exemplary state space trajectories of simulated signals obtained for embedding dimension $D = 2$ and delay time $\tau = 5$ samples.

### 3.3 Adaptive Nonlinear Projective Filtering - Real-Time Implementation

It must be noted that ANPF algorithm, as described in Sec. 3.2 is implementable only for off-line processing of EEG signals. In many practical applications, such as BCI systems, it is required for all utilized algorithms to be causal and realizable in real time (or at least with as short phase delay introduced as possible). Therefore, in this research an implementation of ANPF allowing a causal processing with negligible delay is proposed and validated. This modification will be referred to as ANPF$_{RT}$. For that purpose ANPF algorithm is applied to overlapping segments of analysed signal $x(n)$, each of length $M$. For each discrete time index $n$ filtered output is calculated only from segment $x_m(n) = [x(n-M), x(n-M+1), \ldots, x(n)]$. Resulting, filtered signal $e(n)$ will be delayed for $M$ samples. Described modification of algorithm can be implemented in following steps:

1. for analyzed discrete time index $n$ create a segment $x_m(n) = [x(n-M), x(n-M+1), \ldots, x(n)]$ from past $M-1$ samples of contaminated EEG recording $x(n)$ and current sample;
2. for analyzed discrete time index $n$ create a reference segment $b_{rm}(n) = [b_r(n-M), b_r(n-M+1), \ldots, b_r(n)]$ from past $M-1$ samples of reference signal $b_r(n)$ and current sample;
3. apply ANPF algorithm to $x_m(n)$ with $b_{rm}(n)$ serving as reference to obtain its filtered output $e_n \in \mathbb{R}^M$;
4. filtered output of $x(n)$ at discrete time index $n$ is a first sample of $e_n$: $e(n) = e_n(0)$.

### 3.4 Normalized Least Means Squares Adaptive Filter

An adaptive noise cancelling filter based on NLMS algorithm served as a reference method for validation of ANPF. If $b_{rm}(n) \in \mathbb{R}^M$ is a signal segment extracted from referential EOG recording at time index $n$ consisting of $M$ in a same manner as described in Sec. 3.3, then the output of an adaptive filter at discrete moment $n$ can be calculated as in (5)

$$y(n) = b_{rm}(n)^T w(n). \tag{5}$$

The coefficients $w(n) \in \mathbb{R}^M$ of the filter are being adaptively updated for each new sample. Because of the lack of correlation between desired component $s(n)$ and the reference signal $b_r(n)$ the output $y(n)$ will be fitted to noise component $b(n)$ of $x(n)$. As a result the difference between the filter output at sample $n$ and contaminated signal will be an estimate of desired, uncontaminated signal $s(n)$ as presented in (6)

$$e = x(n) - y(n). \tag{6}$$

The formula for updating the filter coefficients for $n+1$ sample with NLMS algorithm is presented in (7)

$$w(n+1) = w(n) + \mu(n) e(n) b_{rm}(n). \tag{7}$$

The adaptation step in NLMS is normalised with the power of input signal as presented in (8). The purpose of $\gamma$ parameter is to prevent situations where the denominator of that expression approaches 0

$$\mu(n) = \frac{\mu_0}{\gamma + b_{rm}^T(n) b_{rm}(n)}. \tag{8}$$

### 3.5 Testing Procedure

The effectiveness of artifact filtering and correction was evaluated using NMSE measure. Since the data used in this work were simulated, the desired, uncontaminated signal $s(n)$ was available for comparison with filtered discrete time course $e(n)$. The NMSE was calculated for each test as presented in (9).

$$NMSE\big(s(n), e(n)\big) = \frac{\frac{1}{N_0}\sum_{n=1}^{N_0}\big(s(n) - e(n)\big)^2}{\sum_{n=1}^{N_0} s^2(n)} \tag{9}$$

To properly evaluate the effectiveness of proposed ANPF algorithm, assess its advantages and compare it with referential NLMS approach, following tests were designed and performed:

***Test 1*** Sensitivity analysis of ANPF to embedding dimension $D$ from 1 to 12, with fixed delay time $\tau = 10$ samples

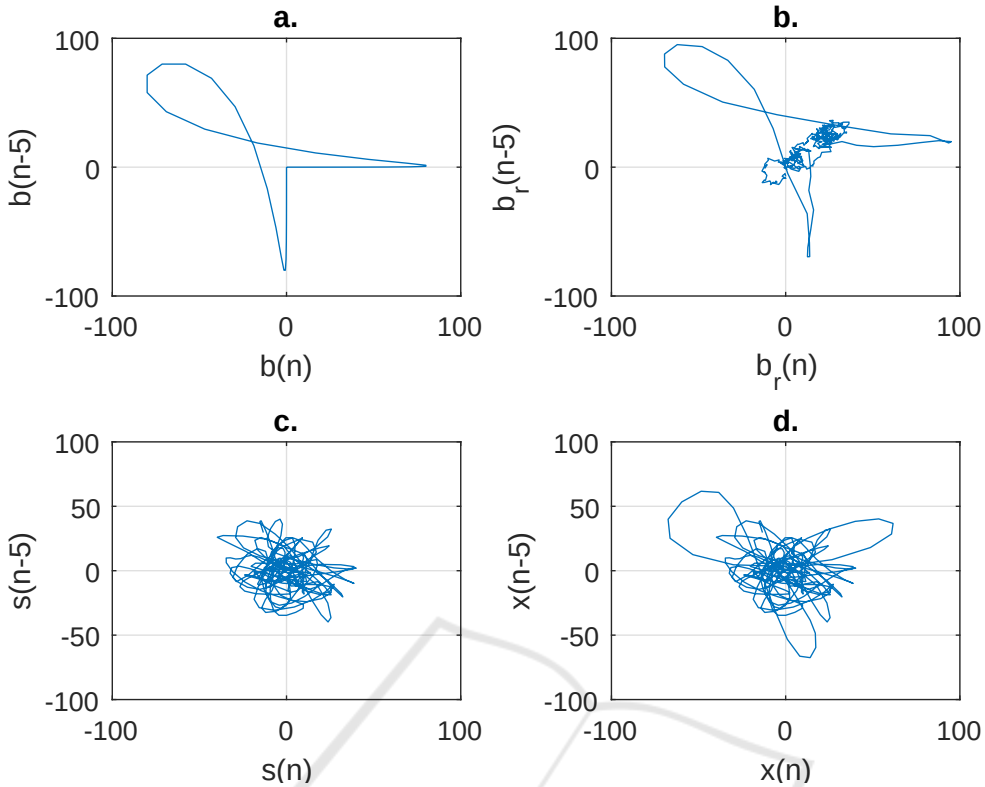


Figure 6: Exemplary state space trajectories of simulated signals: a. eye-blink component; b. reference signal; c. desired EEG component; d. contaminated EEG recording (own source).

***Test 2*** Sensitivity analysis of ANPF to delay time $\tau \in \{1,2,\ldots,40\}$ with embedding dimension $D$ fixed at best value of that parameter selected in *Test 1*

***Test 3*** Sensitivity analysis of NLMS to $\mu_0$ in range $\{0.0001, 0.0002, \ldots, 2.5\}$ with fixed $M = 15$ and $\gamma = 0.01$.

***Test 4*** Sensitivity analysis of NLMS to $M$ in range $\{1,2,\ldots,30\}$ with fixed $\mu_0$ at best value from *Test 3* and $\gamma = 0.01$.

***Test 5*** Comparison between performance of ANPF, ANPF$_{RT}$ and NLMS with parameters ensuring best performance of each method. Range of parameters searched for the best performance of ANPF/ANPF$_{RT}$: $\tau \in \{1,2,\ldots,40\}$, $D \in \{1,2,\ldots,12\}$, $M \in \{1,2,\ldots,30\}$. Range of parameters searched for best performance of NLMS: $\mu_0 \in \{0.0001, 0.0002, \ldots, 2.5\}$, $M \in \{1,2,\ldots,30\}$ and $\gamma = 0.01$.

All of the performed tests consisted of 500 iterations. During each iteration a new, random EEG time course was simulated accordingly to parameters described in Sec. 2. It must be noted, that delay introduced by ANPF$_{RT}$ implementation had to be corrected, so that results obtained with NMSE would remain reliable. However, said correction was implemented during the offline processing. Therefore, it must be taken into account that tests of ANPF$_{RT}$ implementation provide an overview of its correction capabilities rather than real time performance. It must be however noted that the maximal delay that could result from ANPF$_{RT}$ in this research did not exceed 150 ms. The statistical significances of achieved results were evaluated using adequate tests and presented in Sec. 4. To test the differences between mean performances achieved for different configurations of parameters inside each test the one-way analysis of variance (ANOVA) were performed. In such tests the null hypothesis states that samples from different groups are drawn from populations with the same mean against the alternative hypothesis that the population means are not all the same. In this research the grouping is attributed to different parameters in specific sensitivity tests. The desired threshold $\alpha$ value was set to 0.01.

## 4 RESULTS

In Fig. 7 presented are box-plots achieved from *Test 1*. The lowest median NMSE score was obtained for $D = 8$ (marked with green colour in Fig. 7). How-

ever, the one-way ANOVA test performed on the values of this parameter in range from 1 to 9 returned a p-value $p = 0.4442$. Therefore, it can be concluded that for this range of $D$ parameter no significant differences between mean NMSE occurred. After some threshold value is exceeded (in this work for $D_{lim} = 9$) algorithm's performance begins to downgrade.

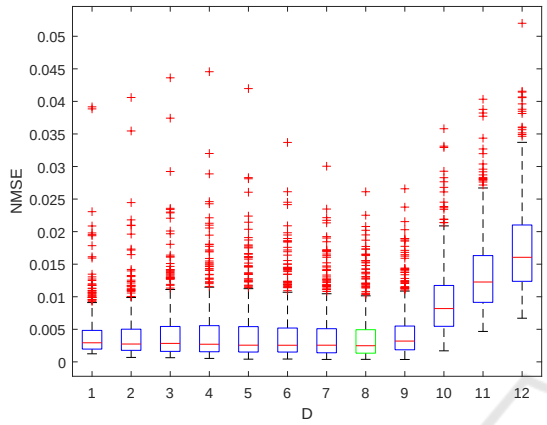


Figure 7: Analysis of ANPF algorithm's sensitivity to embedding dimension $D$ parameter (own source).

Presented in Fig. 8 are box-plots achieved from *Test 2*. To ensure a clear overview of performed test only selected values of $\tau$ were included. The lowest median NMSE score was obtained for $\tau = 10$ (marked with green colour in Fig. 8). The one-way ANOVA test performed for $\tau \in \{1, 2, \ldots, 11\}$ returned a $p = 0.1138$, which is higher than desired $\alpha = 0.01$. Therefore, it can be concluded that for lower values of $\tau$ differences in performance are not significant. Similar behaviour can be observed for $\tau \in \{19, 20, \ldots, 40\}$. The p-value obtained for that group was also greater than 0.01 ($p = 0.4167$). It can be observed that as $\tau$ exceeds some limit the performance start to decrease and then stabilizes at steady level, where it is

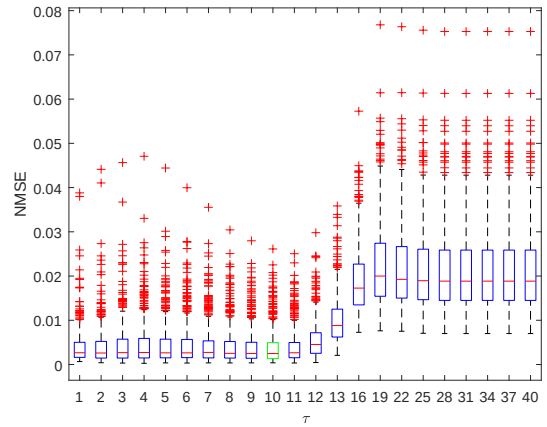


Figure 8: Analysis of ANPF algorithm's sensitivity to delay time $\tau$ (own source).

no longer affected by increases of $\tau$.

In Fig. 9 presented are selected box-plots achieved from *Test 3*. The lowest median NMSE score was obtained for $\mu_0 = 0.1$ (marked with green colour in Fig. 7). Visual inspection of result reveals the possibility of means being equal in two groups: $\mu_0 = 0.0001 \div 0.001$ and $\mu_0 = 0.1 \div 1.9$. One-way ANOVA tests of each group returned respectively $p = 0.3196$ and $p = 0.1365$. According to achieved results overall mean NMSE tends to decrease with the increase of $\mu_0$. Then, for a great range of $\mu_0$ values the NMSE remains stable until a value is reached when the filtering error becomes very high. To maintain the clarity of a data presentation, results for $\mu_0 > 2.0$ were not included. In other words, best $\mu_0$ value needs to be individually selected for each specific case as it is not related to neither high nor low values of $\mu_0$. This observation corresponds well with general knowledge about characteristics of adaptive filters (Haykin and Widrow, 2003).

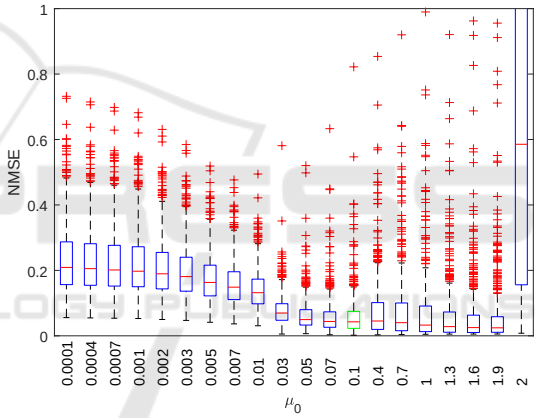


Figure 9: Analysis of NLMS algorithm's sensitivity to adaptation step $\mu$ (own source).

In Fig. 10 presented are box-plots achieved from *Test 4*. The lowest median NMSE score was obtained for $M = 2$ (marked with green colour in Fig. 10). For $M = 13 \div 30$ calculated p-value ($p = 0.0456$) exceeds desired $\alpha$ which indicates that NLMS is not sensitive to changes of that parameter in that range in described case. It is worth noting that for lower values of $M$ a better performance was achieved.

Fig. 11 presents the comparison between fine-tuned off-line ANPF, ANPF$_{RT}$ (with delay correction) and NLMS. Lowest median of NMSE for all test repetitions $ANPF_{med} = 0.0025$ was achieved for ANPF with embedding dimension $D = 8$ and delay $\tau = 10$. Real time implementation ANPF$_{RT}$ obtained median NMSE score $ANPF_{RT_{med}} = 0.0043$ for parameters $D = 2$, $\tau = 1$ and $M = 30$. Referential method based on NLMS adaptive filter algorithm allowed to achieve median NMSE $NLMS_{med} = 0.004$. Since

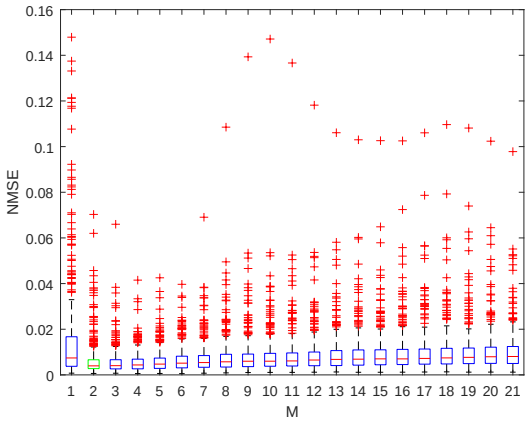


Figure 10: Analysis of NLMS algorithm's sensitivity to filter length $M$ (own source).

differences between performances of methods were compared with one-vs-one strategy, one-way ANOVA tests have been replaced with two sample t-tests. All differences revealed to be statistically significant (p-values of $e-09$ range). Therefore, it can be concluded that correction quality of proposed ANPF algorithm significantly outperforms referential NLMS algorithm. Additionally, it can be observed that real time implementation of ANPF downgrades its performance, event with the correction of phase delay. Thus, NLMS remains a better choice for real time applications.

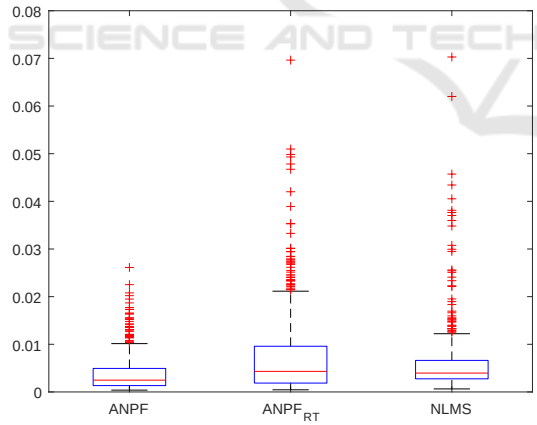


Figure 11: Comparison between fine-tuned ANPF, ANPF$_{RT}$ (with delay correction) and NLMS (own source).

## 5 CONCLUSIONS

In this work a concept of a novel approach to adaptive filtering of eye blink related artifacts from EEG signals was presented and validated. ANPF algorithm achieved a highly satisfactory performance during conducted tests. The median NMSE score achieved by ANPF in described experiment has significantly outperformed referential method based on NLMS algorithm (0.0025 to 0.004). Additionally, during sensitivity analysis it was revealed that ANPF algorithm is robust to changes of its parameters, especially in lower ranges of their values. As a result, utilization of proposed algorithm for analysis of EEG signals becomes easier and less demanding from the parameter selection perspective. This stands in great contrast to popularly used adaptive filters based on least mean squares algorithms. Such algorithms are known to be highly dependent on their parameters and may even become unstable due to their poor selection. This behaviour was observed also in this work. On the other hand, it should be noted that in case of this research, performed tests focused on the artifact filtering and correction effectiveness of presented methods. Since the original form of ANPF is designed for off-line use and its real time implementation ANPF$_{RT}$ required the off-line correction of the phase delay, it is obvious that they are less suited for real time applications than NLMS. This conclusion is furtherly supported by the observed downgrade of ANPF algorithm's effectiveness in its real time implementation ANPF$_{RT}$. The best performance of ANPF$_{RT}$ was achieved with relatively low delay of 150 $ms$. Additionally, the NLMS based approach outperformed ANPF$_{RT}$ 0.004 to 0.0043 in terms of median NMSE. Although the difference is not great, it tested to be statistically significant. However, this fact should not cover the superiority of generic ANPF algorithm for off-line filtering of EEG signals.

## ACKNOWLEDGEMENTS

This work was supported by Silesian University of Technology grant no. 02/010/BKM16/0047/31 and BK/213/RAu1/2016. The research presented here was funded by the Silesian University of Technology grant BK for Institute of Automatic Control (for both Data Mining and Control and Robotics Groups) for 2017 year. Moreover, the calculations were performed with the use of IT infrastructure of GeCONiI Upper Silesian Centre for Computational Science and Engineering (NCBiR grant no POIG.02.03.01-24-099/13)

## REFERENCES

Benedetto, S., Pedrotti, M., Minin, L., Baccino, T., Re, A., and Montanari, R. (2011). Driver workload and eye

blink duration. *Transportation Research Rart F: Traffic Psychology and Behaviour*, 14(3):199–208.

Binias, B., Myszor, D., Niezabitowski, M., and Cyran, K. A. (2016a). Evaluation of alertness and mental fatigue among participants of simulated flight sessions. In *Carpathian Control Conference (ICCC), 2016 17th International*, pages 76–81. IEEE.

Binias, B., Palus, H., and Jaskot, K. (2015). Real-time detection and filtering of eye movement and blink related artifacts in EEG. In *2015 20th International Conference on Methods and Models in Automation and Robotics (MMAR)*, pages 903–908. IEEE.

Binias, B., Palus, H., and Jaskot, K. (2016b). Real-time detection and filtering of eye blink related artifacts for brain-computer interface applications. In *Man–Machine Interactions 4*, pages 281–290. Springer.

Blankertz, B., Tomioka, R., Lemm, S., Kawanabe, M., and Muller, K.-R. (2008). Optimizing spatial filters for robust EEG single-trial analysis. *IEEE Signal Processing Magazine*, 25(1):41–56.

Correa, A. G., Laciar, E., Patiño, H., and Valentinuzzi, M. (2007). Artifact removal from EEG signals using adaptive filters in cascade. 90(1):012081.

Craig, A., Tran, Y., Wijesuriya, N., and Nguyen, H. (2012). Regional brain wave activity changes associated with fatigue. *Psychophysiology*, 49(4):574–582.

da Silva, F. L. (1991). Neural mechanisms underlying brain waves: from neural membranes to networks. *Electroencephalography and Clinical Neurophysiology*, 79(2):81–93.

Gao, J., Hu, J., and Tung, W.-w. (2011). Facilitating joint chaos and fractal analysis of biosignals through nonlinear adaptive filtering. *PloS one*, 6(9):e24331.

Grunwald, M., Weiss, T., Krause, W., Beyer, L., Rost, R., Gutberlet, I., and Gertz, H.-J. (1999). Power of theta waves in the EEG of human subjects increases during recall of haptic information. *Neuroscience Letters*, 260(3):189–192.

Harezlak, K. (2017). Eye movement dynamics during imposed fixations. *Information Sciences*, 384:249 – 262.

Haykin, S. and Widrow, B. (2003). *Least-mean-square adaptive filters*, volume 31. John Wiley & Sons.

Jung, T.-P., Makeig, S., Humphries, C., Lee, T.-W., Mckeown, M. J., Iragui, V., and Sejnowski, T. J. (2000). Removing electroencephalographic artifacts by blind source separation. *Psychophysiology*, 37(2):163–178.

Kantz, H. and Schreiber, T. (1998). Nonlinear projective filtering I: background in chaos theory. *arXiv preprint chao-dyn/9805024*.

Kotas, M. (2004). Projective filtering of time-aligned ECG beats. *IEEE Transactions on Biomedical Engineering*, 51(7):1129–1139.

Kotas, M. (2009). *Nonlinear projective filtering of ECG signals*. INTECH Open Access Publisher.

Makeig, S., Bell, T., Lee, T., Jung, T., Enghoff, S., et al. (2000). EEGLAB: ICA toolbox for psychophysiological research. *WWW Site, Swartz Center for Computational Neuroscience, Institute of Neural Computation, University of San Diego California*.

Nunez, P. L. and Srinivasan, R. (2006). *Electric fields of the brain: the neurophysics of EEG*. Oxford university press.

Nunez, P. L., Srinivasan, R., Westdorp, A. F., Wijesinghe, R. S., Tucker, D. M., Silberstein, R. B., and Cadusch, P. J. (1997). EEG coherency: I: statistics, reference electrode, volume conduction, Laplacians, cortical imaging, and interpretation at multiple scales. *Electroencephalography and Clinical Neurophysiology*, 103(5):499–515.

P. Berg, M. S. (1991). Dipole models of eye activity and its application to the removal of eye artifacts from the EEG ad MEG. *Clinical Physics and Physiological Measurements*, 12:49–54.

Pfurtscheller, G. and Da Silva, F. L. (1999). Event-related EEG/MEG synchronization and desynchronization: basic principles. *Clinical Neurophysiology*, 110(11):1842–1857.

R. J. Croft, R. J. B. (2000). Removal of ocular artifact from the EEG: a review. *Clinical Neurophysiology*, 30:5–19.

Richter, M., Schreiber, T., and Kaplan, D. T. (1998). Fetal ECG extraction with nonlinear state-space projections. *IEEE Transactions on Biomedical Engineering*, 45(1):133–137.

Schreiber, T. and Kantz, H. (1998). Nonlinear projective filtering I: Application to real time series. *arXiv preprint chao-dyn/9805025*.

Takens, F. (1981). Detecting strange attractors in turbulence. In *Dynamical systems and turbulence, Warwick 1980*, pages 366–381. Springer.

Teplan, M. (2002). Fundamentals of EEG measurement. *Measurement Science Review*, 2(2):1–11.